

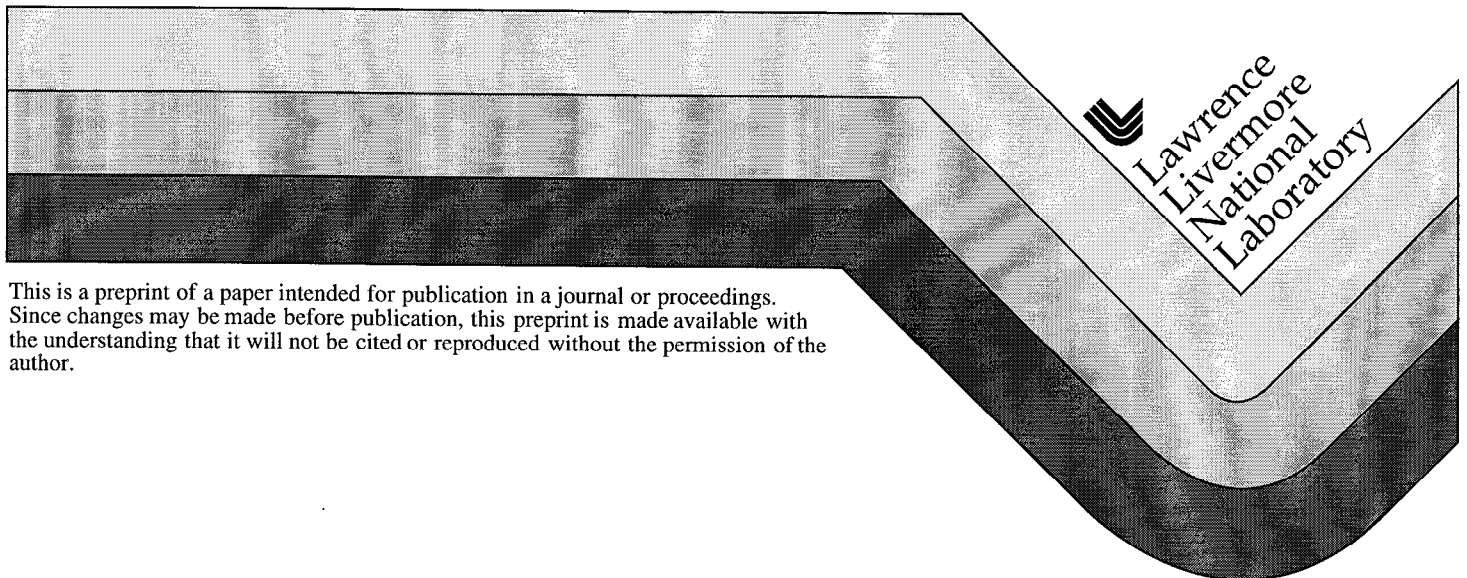
UCRL-JC-134740  
PREPRINT

# **Ion Detection with a Cryogenic Detector Compared to a Microchannel Plate Detector in MALDI TOF-MS**

G. Westmacott  
F. Zhong  
M. Frank  
S. Labov  
W.H. Benner

This paper was prepared for submittal to the  
47th American Society for Mass Spectrometry Conference on Mass Spectrometry  
and Applied Topics

**June 1999**



This is a preprint of a paper intended for publication in a journal or proceedings.  
Since changes may be made before publication, this preprint is made available with  
the understanding that it will not be cited or reproduced without the permission of the  
author.

#### DISCLAIMER

This document was prepared as an account of work sponsored by an agency of the United States Government. Neither the United States Government nor the University of California nor any of their employees, makes any warranty, express or implied, or assumes any legal liability or responsibility for the accuracy, completeness, or usefulness of any information, apparatus, product, or process disclosed, or represents that its use would not infringe privately owned rights. Reference herein to any specific commercial product, process, or service by trade name, trademark, manufacturer, or otherwise, does not necessarily constitute or imply its endorsement, recommendation, or favoring by the United States Government or the University of California. The views and opinions of authors expressed herein do not necessarily state or reflect those of the United States Government or the University of California, and shall not be used for advertising or product endorsement purposes.



# Ion Detection with a Cryogenic Detector Compared to a Microchannel Plate Detector in MALDI TOF-MS

G. Westmacott<sup>1</sup>, F. Zhong<sup>1</sup>, M. Frank<sup>2</sup>, S. Labov<sup>2</sup>, W.H. Benner<sup>1</sup>

<sup>1</sup>Lawrence Berkeley National Laboratory, MS 70A-3363, 1 Cyclotron Road, Berkeley, CA 94720

<sup>2</sup>Lawrence Livermore National Laboratory, PO Box 808, MS L-418, Livermore, CA 94551

Detection of molecular ions in mass spectrometry is typically accomplished by an ion colliding with a surface and then amplifying the emitted secondary electrons. It is well established that the secondary electron yield decreases as the mass of the primary ion increases [1-3], thus limiting the detection efficiency of large molecular ions. One way around this limitation is to use secondary ion detectors because the emission efficiency of secondary ions does not seem to decrease for increasing primary ion mass [1]. However this technique has limitations in timing resolution because of the mass spread of the emitted secondary ions. To find other ways around high mass detection limitations it is important to understand existing mechanisms of detection and to explore alternative detector types. To this end, a superconducting tunnel junction (STJ) detector was used in measuring the secondary electron emission efficiency,  $\varepsilon_e$ , for a MCP detector. STJ detectors are *energy sensitive* and do not rely on secondary emission to produce a signal.

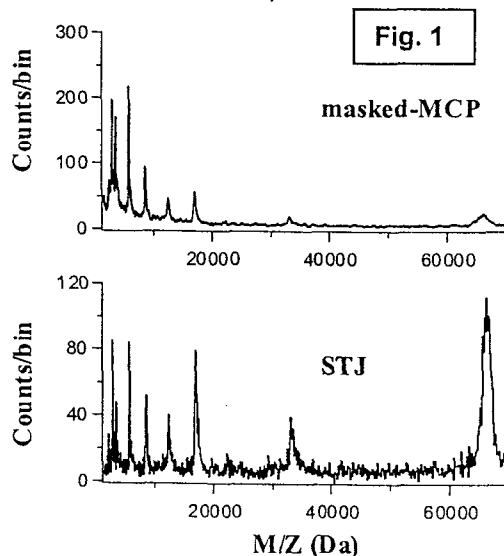
Using a linear MALDI-TOF mass spectrometer, a STJ detector is mounted directly behind the hole in an annular MCP detector. This mounting arrangement allows ions to be detected simultaneously by each detector. The STJ detector sits in a liquid helium cryostat and is operated at 1.3 K to minimize thermal noise (see [4,5] for more details). Primary ions passing through the center hole of the MCP detector collide with the 0.04 mm<sup>2</sup> STJ surface and generate a detector-pulse that is approximately proportional to the ion's total energy. A mask with a small hole in it was placed in front of the MCP detector so that the MCP and STJ detectors have approximately the same effective active areas. The ion beam diameter near the MCP is over 2.5 cm (measured with a MCP-phosphorus screen detector) and the axial separation of the two detectors is about 4 mm. Both detectors were operated in pulse-counting mode and set to have the same effective deadtime.

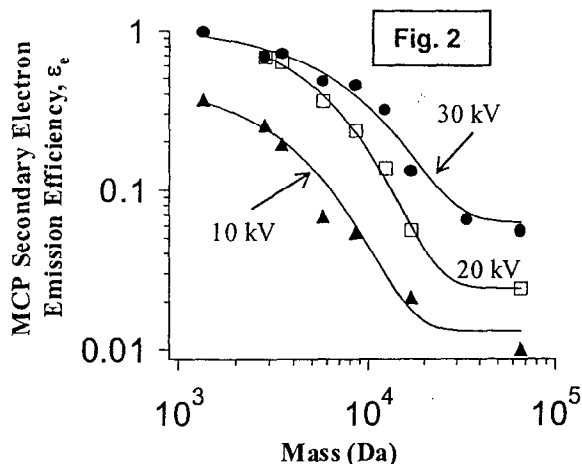
Fig. 1 shows a comparison between the mass spectra acquired with the masked-MCP detector and the STJ detector. For increasing mass, the efficiency of the MCP detector decreases, whereas the efficiency of the energy-sensitive STJ detector remains at 100%; there is no loss in sensitivity for detecting larger mass ions. In fact, for masses above ~2000 Da, the amplitude of the signal from the STJ increases for increasing mass (figure not shown).

The detection efficiency,  $\varepsilon_{\text{det}}$ , for the masked MCP is determined for each molecular ion species by dividing the MCP counts by the STJ counts and normalizing this ratio such that it is unity for substance P at 30 keV. The secondary electron emission efficiency,  $\varepsilon_e$ , which is the probability that one or more electrons is emitted from a surface bombarded by exactly one primary ion, can be calculated by using the following equation:

$$\varepsilon_{\text{det}} = 1 - \sum_{n=1}^3 K_n (1 - \varepsilon_e)^n$$

where  $K_n$  is the measured multiplicity of primary ions striking each detector. Pulse height analysis of the signal from the STJ detector (not shown) gives  $K_n$ . On average, ~77% of all detection events are from one molecular ion hitting the detector ( $K_1$ ), and  $K_2 \approx 17\%$  and  $K_3 \approx 6\%$ . The masked-MCP and STJ detector have approximately the same effective areas, thus the coefficients  $K_n$  from the STJ detector are



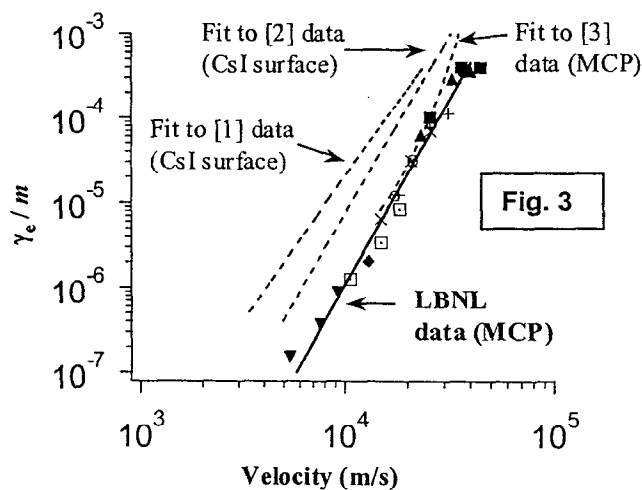


approximately the same for the MCP detector. There are very few events where more than 3 ions simultaneously strike the detector, thus the series was truncated at  $n = 3$ . Higher order terms would slightly reduce  $\epsilon_e$ .

The results for  $\epsilon_e$  plotted as a function of mass for three different accelerating voltages are shown in Fig. 2. A general exponential function  $A + B \exp(-C m)$  was fit to each data set as a guide for the eye. Using all the data in Fig. 2 and assuming a Poisson distribution for the multiplicity of emitted secondary electrons, the average number of secondary electrons,  $\gamma_e$ , can be calculated.

In Fig. 3,  $\gamma_e/m$  is plotted as a function of ion velocity and the data was fit to  $\gamma_e/m = Av^B$ , where  $m$  is the mass,  $v$  is the velocity, and  $B$  was found to be  $4.3 \pm 0.4$ . The data points in Fig. 3 correspond to ● substance P, ■ melittin, ▲ glucagon, + insulin, × ubiquitin, ○ cytochrome C, □ apomyoglobin, ◆ apomyoglobin [2M+H]<sup>+</sup>, and ▼ albumin. Our results are compared in Fig. 3 to previously published results. The MCP secondary electron yield appears to be about a factor of 4 lower than the CsI conversion surfaces [1,2], however the slope of all the data is consistent and shows a steep velocity dependence with no velocity threshold at least down to 5 km/s for the emission of secondary electrons. Our measurements extend previous measurements made for the MCP surface [3].

The unique feature of the STJ detector is that it is energy sensitive. The STJ detectors are 100% efficient as long as the ion's energy is above the electronic noise level (~5 keV in our measurements). There is no loss in sensitivity for increasing ion mass, in contrast to secondary electron emission detectors. This feature can be used to investigate certain fundamental aspects of mass spectrometry, for example, the measurements shown here, or investigating the energetics involved with ion-surface collisions.



For the STJ detector, the small size and operation at low temperatures limits its practicality for routine mass spectrometry. However, these limitations will soon be reduced with the development of cryogenic detector arrays and close-cycle coolers.

This work was supported by the Director, Office of Energy Research, Office of Health and Environmental Research, Human Genome Program, U.S. Department of Energy under contract number DE-AC03-76SF00098, and also performed under the auspices of the U.S. Department of Energy by LLNL under contract number W-7405-ENG-48.

- [1] G. Westmacott, W. Ens, K.G. Standing, *Nucl. Instr. and Meth.*, **B 108** (1996) 282.
- [2] A. Brunelle, P. Chaurand, S. Della-Negra, Y. Le Beyec, E. Parilis, *Rapid Commun. Mass Spectrom.*, **11** (1997) 353.
- [3] P.W. Geno, R.D. Macfarlane, *Int. J. Mass Spectrom. Ion Process.* **92** (1989) 195.
- [4] W.H. Benner, D.M. Horn, J.M. Jaklevic, M. Frank, C. Mears, and S. Labov, *J. Am. Soc. Spectrom.*, **8** (1997) 1094.
- [5] M. Frank, S. Labov, W.H. Benner, and G. Westmacott, submitted to *Mass Spectrom. Rev.*, 1999.

**1**

## OVERVIEW

### PURPOSE

- Compare the response of a MCP detector to a superconducting tunnel junction (STJ) detector
- Measure the secondary electron emission efficiency,  $\epsilon_e$ , and determine the secondary electron yield,  $\gamma_e$ , for the MCP detector

### METHOD

- Bombard detectors with MALDI ions
- Detect ions by pulse-counting using, simultaneously, a STJ and an annular MCP detector

### RESULTS

- For the STJ detector there is *no loss of detection sensitivity for increasing mass* as there is for secondary electron emission detectors
- For the MCP, the secondary electron yield can be expressed as  $\gamma_e = Amv^B$  where  $B \approx 4.3$
- Also for the MCP, observed *no velocity threshold* for primary ions with velocities  $> 5$  km/s.

**2**

## INTRODUCTION

Detection of molecular ions in mass spectrometry is typically accomplished by colliding molecular ions into a surface and amplifying the signal generated by secondary electrons.

It is well established that the secondary electron yield decreases as the mass of the primary ion increases [1-3], thus limiting the detection efficiency of large molecular ions. One way around this limitation is to use secondary ion detectors, where the efficiency does not seem to decrease for increasing primary ion mass [1].

In order to explore other ways around high mass detection limitations, it is important to both understand existing mechanisms of detection and to explore alternative detector types.

The secondary electron emission efficiency,  $\epsilon_e$ , was measured for a MCP detector. This was done by normalizing the number of MCP counts (detection events) to that measured a *super-conducting tunnel junction (STJ) detector*. STJ detectors are energy sensitive and do not rely on secondary emission to produce a signal. The secondary electron yield,  $\gamma_e$ , was calculated from  $\epsilon_e$ .

3

## EXPERIMENTAL

The experimental setup is shown in FIGURE 1.

A STJ detector is mounted directly behind the hole in an annular MCP detector. This mounting arrangement allows ions to be detected simultaneously by each detector.

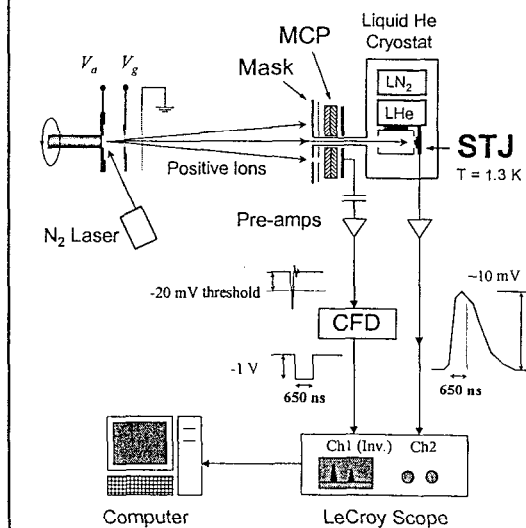
The STJ detector sits in a liquid helium cryostat and is operated at 1.3 K to minimize thermal noise. (See [4,5] for more details.) Primary ions passing through the center hole of the MCP detector collide with the 0.04 mm<sup>2</sup> STJ surface and generate a detector-pulse whose height is approximately proportional to the ion's total energy.

To compare the STJ and MCP detectors, a mask with a small hole in it was placed in front of the MCP detector so that the MCP and the STJ detectors have approximately the same effective active areas.

Both detectors were operated in *pulse-counting mode* and set to have the same effective deadtime.

4

FIGURE 1: Experimental setup



5

## RESULTS

### STJ Detector Performance

The upper graph in FIGURE 2 shows a scatter plot of the STJ detector pulse height vs. flight time. Each point represents a single detection event. Below this scatter plot is the corresponding TOF spectrum. FIGURE 3 shows a pulse height histogram of the STJ detector signal for insulin and myoglobin.

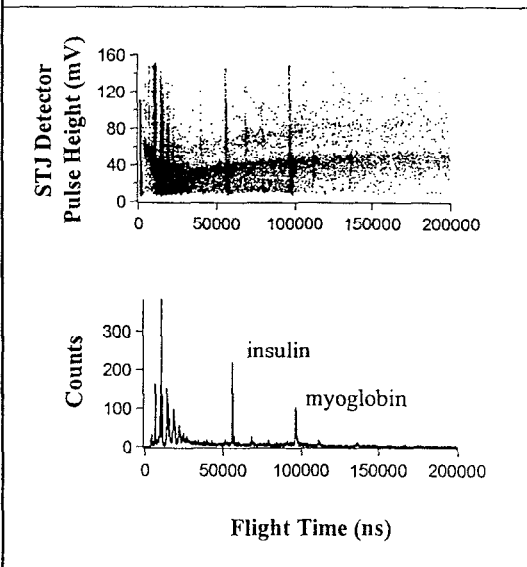
In FIGURE 3, the predominant lower energy peaks correspond to events where *exactly 1* primary ion hits the STJ detector. About 77% of all detection events occur with a single ion collision. Likewise, the next smaller peak at about twice the energy corresponds to *exactly 2* ions; this happens ~17% of the time. There could also be a small (negligible) contribution from doubly charged dimers. *Since the masked-MCP has about the same effective area as the STJ, it has approximately the same multiplicity of primary ions hitting it.*

FIGURE 3 also shows a slight increase in the measured energy for myoglobin (with lower velocity) relative to insulin. This trend is plotted in FIGURE 4 for other masses. For increasing mass, the STJ detector pulse height passes through a minimum at approximately 2000 Da. For constant accelerating voltage, the *STJ detector pulse height does not decrease for increasing mass* as does the yield of secondary electrons.

6

FIGURE 2: Sample STJ TOF spectrum.

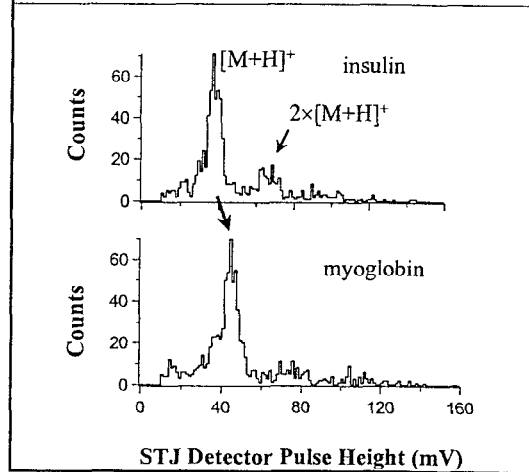
$V_a = 30$  kV.



7

**FIGURE 3:** Sample STJ pulse height spectra.  $V_a = 30$  kV.

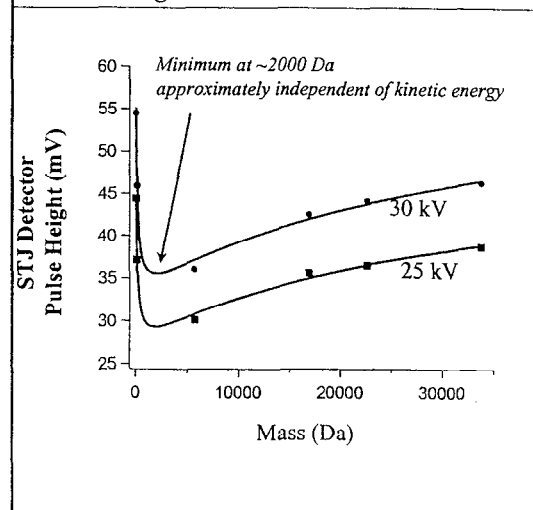
- Note the *shift to higher signal amplitude* for myoglobin & the multiplicity of primary ions hitting the detector.



8

**FIGURE 4:** STJ detector pulse height vs. mass.

- There is *no loss in sensitivity* for increasing mass.



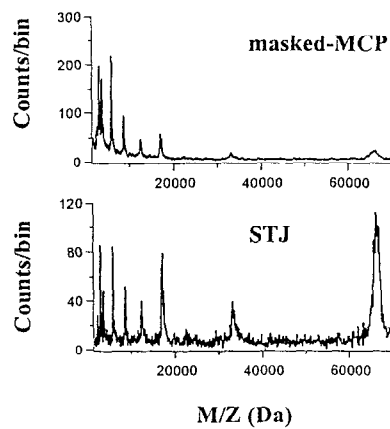
9

### Masked-MCP vs STJ Detector

FIGURE 5 shows a comparison between the mass spectrum acquired with the masked-MCP detector and the STJ detector. For increasing mass, the efficiency of the MCP detector decreases, whereas the efficiency of the energy-sensitive STJ detector remains at 100%. Because of the detection mechanism, this is expected.

10

FIGURE 5: Comparison between the STJ and MCP detectors.  $V_a = 30$  kV.



11

### Secondary Electron Emission Efficiency, $\epsilon_e$

The *detection efficiency*,  $\epsilon_{\text{det}}$ , for the masked-MCP is determined for each molecular ion species by dividing the MCP counts by the STJ counts and normalizing this ratio such that it is unity for substance P at 30 keV.

The *secondary electron emission efficiency*,  $\epsilon_e$ , is defined as the probability that 1 or more electrons is produced by the impact of *exactly 1* molecular ion.

$\epsilon_e$  can then be calculated by using the known *multiplicity*,  $K_n$ , of primary ions striking each detector (as shown in FIGURE 3) in the following equation:

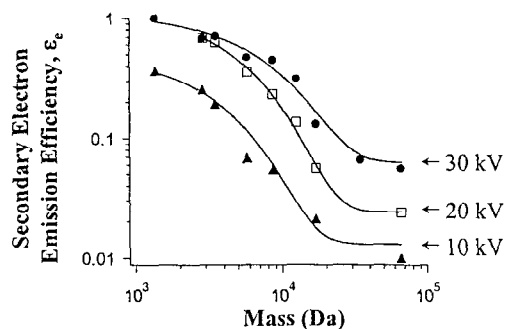
$$\epsilon_{\text{det}} = 1 - \sum_{n=1}^3 K_n (1 - \epsilon_e)^n$$

The number of events where more than 3 ions simultaneously strike the detector is very small. Thus this series can be truncated at  $n = 3$  ions. The results for  $\epsilon_e$  are shown in FIGURE 6.

12

**FIGURE 6:** Secondary electron emission efficiency,  $\epsilon_e$ , for the MCP detector.  $V_a = 30, 20,$  and  $10$  kV.

- Data is fit to  $A + B \exp(-Cm)$  as a guide for the eye.



13

### Secondary Electron Yield, $\gamma_e$

The average number of secondary electrons,  $\gamma_e$ , can be calculated for all the  $\epsilon_e$  data plotted in FIGURE 6 by assuming a Poisson distribution for the secondary electron multiplicity.

In FIGURE 7  $\gamma_e / m$  is plotted as a function of ion velocity. The data was fit to

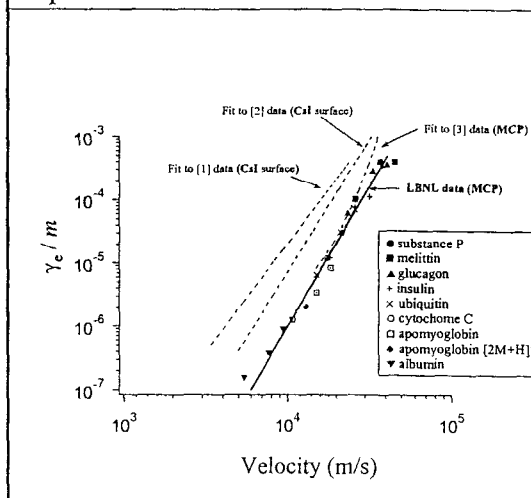
$$\frac{\gamma_e}{m} = Av^B$$

where  $m$  is the mass,  $v$  is the velocity, and  $B$  was found to be  $4.3 \pm 0.4$ .

Our results are compared in FIGURE 7 to previously published results. The MCP secondary electron yield,  $\gamma_e$ , appear to be a factor of  $\sim 4$  lower than the CsI conversion surfaces. The slope of all the data is consistent and shows a steep velocity dependence. Furthermore, our measurements extend previous measurements made for the MCP surface. There is no observed velocity threshold for the MCP detectors for primary ions with velocity  $> 5$  km/s.

14

**FIGURE 7:** Reduced secondary electron yield,  $\gamma_e / m$ , for the MCP detector compared to previously published results.



15

### Overall Detection Efficiency

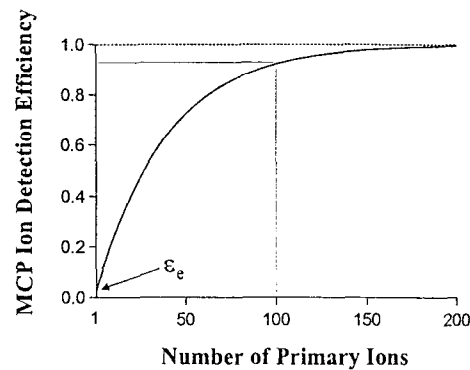
Overall ion detection efficiency depends both on the probability that an ion will strike the detector *and* the probability that an impacting ion will generate a signal (not taking into account the background signal). For the STJ detector the probability that an impacting 30 keV ion will generate a signal is 100%, however, its small size (0.04 mm<sup>2</sup>) limits its overall detection efficiency. Because of its size, it is necessary to average thousands of single spectra to generate a final spectrum with reasonable statistics. Each spectrum for this experiment was generated from ~5000 laser shots.

One obvious advantage of the MCP detector is its large active area. This greatly reduces the number of laser shots needed to acquire reasonable statistics. Furthermore, even though the secondary electron emission efficiency may be low for, say, albumin (66 kDa) at 30 keV, with  $\epsilon_e = 5\%$ , the probability of detecting it increases with an increasing number of ions hitting the detector. This is illustrated by the graph in FIGURE 8. Assuming a 50% MCP open area ratio (the ratio of active to non-active surface), for 100 ions striking the detector, the overall detection efficiency is greater than 90%.

16

**FIGURE 8:** MCP detection efficiency for albumin (66 kDa) at 30 keV.

- Assuming a 50% MCP open area ratio.
- Detection efficiency rapidly increases for increasing number of primary ions.



17

## CONCLUSION

The *secondary electron yield* was determined for large, slow moving molecular ions incident on a MCP. Our results extend previous measurements [3] and show no primary ion velocity threshold ( $> 5$  km/s) for secondary electron emission. Furthermore, the secondary electron yield,  $\gamma_e$ , decreases with velocity to roughly the 4<sup>th</sup> power. Our results are consistent with previous measurements using CsI converters [1,2], however  $\gamma_e$  appears to be a factor of  $\sim 4$  lower for the MCP than for CsI conversion surfaces.

*The unique feature of the STJ detector* is that it is energy sensitive. The STJ detectors are 100% efficient as long as the ion energy is above the electronic threshold ( $\sim 5$  keV in our measurements). There is no loss in sensitivity for increasing ion mass, in contrast to secondary emission detectors. This feature can be used to investigate certain fundamental aspects of mass spectrometry, for example, the measurements in this experiment, or investigating the energetics involved with ion-surface collisions.

*In the Future:* For the STJ detector, the small size and operation at low temperatures (1.3 K) limits its practicality for routine mass spectrometry. However, these limitations will soon be reduced with the development of cryogenic detector arrays and close-cycle coolers.

18

## REFERENCES

- [1] G. Westmacott, W. Ens, K.G. Standing, *Nucl. Instr. And Meth.*, **B 108** (1996) 282.
- [2] A. Brunelle, P. Chaurand, S. Della-Negra, Y. Le Beyec, E. Parilis, *Rapid Commun. Mass Spectrom.*, **11** (1997) 353.
- [3] P.W. Geno, R.D. Macfarlane, *Int. J. Mass Spectrom. Ion Process.* **92** (1989) 195.
- [4] W.H. Benner, D.M. Horn, J.M. Jaklevic, M. Frank, C. Mears, and S. Labov, *J. Am. Soc. Spectrom.*, **8** (1997) 1094.
- [5] M. Frank, S. Labov, W.H. Benner, and G. Westmacott, submitted to *Mass Spectrom. Rev.*, 1999.